

Discovery of a Potent, Injectable Inhibitor of Aurora Kinases Based on the Imidazo-[1,2-*a*]-Pyrazine Core

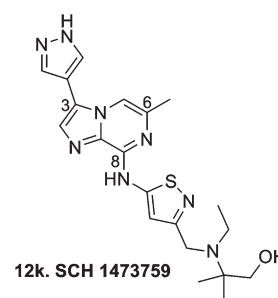
Tao Yu,<sup>†</sup> Jayaram R. Tagat,<sup>\*†</sup> Angela D. Kerekes,<sup>†</sup> Ronald J. Doll,<sup>†</sup> Yonglian Zhang,<sup>†</sup> Yushi Xiao,<sup>†</sup> Sara Esposito,<sup>†</sup> David B. Belanger,<sup>†</sup> Patrick J. Curran,<sup>†</sup> Amit K. Mandal,<sup>†</sup> M. Arshad Siddiqui,<sup>†</sup> Neng-Yang Shih,<sup>†</sup> Andrea D. Basso,<sup>§</sup> Ming Liu,<sup>§</sup> Kimberly Gray,<sup>§</sup> Seema Tevar,<sup>§</sup> Jennifer Jones,<sup>§</sup> Suining Lee,<sup>§</sup> Lianzhu Liang,<sup>§</sup> Samad Ponery,<sup>§</sup> Elizabeth B. Smith,<sup>§</sup> Alan Hruza,<sup>||</sup> Johannes Voigt,<sup>||</sup> Lata Ramanathan,<sup>||</sup> Winifred Prorise,<sup>||</sup> and Mengwei Hu<sup>⊥</sup>

Departments of <sup>†</sup>Chemical Research, <sup>§</sup>Oncology, <sup>||</sup>Structural Chemistry and <sup>⊥</sup>Pharmaceutical Sciences  
Merck Research Laboratories, 2015 Galloping Hill Road, K-15-2B-2800, Kenilworth, New Jersey 07033,

<sup>\*</sup>Department of Chemical Research, Merck Research Laboratories, 320 Bent Street, Cambridge, Massachusetts 02141

**ABSTRACT** The imidazo-[1,2-*a*]-pyrazine (**1**) is a dual inhibitor of Aurora kinases A and B with modest cell potency ( $IC_{50} = 250$  nM) and low solubility ( $5 \mu\text{M}$ ). Lead optimization guided by the binding mode led to the acyclic amino alcohol **12k** (SCH 1473759), which is a picomolar inhibitor of Aurora kinases (TdF  $K_d$  Aur A = 0.02 nM and Aur B = 0.03 nM) with improved cell potency (phos-HH3 inhibition  $IC_{50} = 25$  nM) and intrinsic aqueous solubility (11.4 mM). It also demonstrated efficacy and target engagement in human tumor xenograft mouse models.

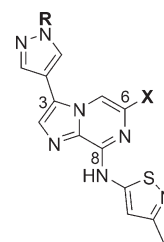
**KEYWORDS** Aurora kinase inhibitors, cell potency, aqueous solubility, imidazo-[1,2-*a*]-pyrazine, tumor xenograft model, SCH 1473759



The Aurora kinases are a family of three Ser/Thr kinases that play a critical role during the mitotic stage of the cell cycle. They are overexpressed in a range of tumors, which suggests that they could be promising targets for cancer therapy.<sup>1</sup> Several Aurora kinase inhibitors are currently undergoing clinical evaluation.<sup>2</sup> Aurora kinases A and B are highly homologous and seem to work in concert during mitosis. Aurora kinase A is involved in mitotic entry and bipolar spindle assembly. Inhibition of Aurora A results in mitotic delay and formation of monopolar spindle phenotype followed by cell death. Early in mitosis, Aurora B phosphorylates histone H3 on Ser10 (phos-HH3) and later in mitosis regulates cell division. Aurora B is also a key component of the mitotic spindle checkpoint. Inhibition of Aurora B results in aberrant endoreduplication and abrogation of cytokinesis, leading to apoptosis. When both Aurora kinases A and B are inhibited, the dominant phenotype is the one resulting from the inhibition of Aurora B.<sup>3</sup> Selective inhibitors of either one of the isoforms as well as dual inhibitors of both Aurora kinases A and B have been reported.<sup>4–6</sup> While designing potent kinase inhibitors guided by an X-ray structure of a ligand-bound form of the enzyme has become common practice,<sup>7,8</sup> optimizing such a lead to improve its druglike properties still depends on traditional approaches. Herein, we describe a combination of rational and traditional efforts to optimize the lead structure **1** (Table 1)<sup>9</sup> with the goal of improving its cell potency, pharmacokinetics (PK), and aqueous solubility suitable for an intravenous formulation.

The early efforts that identified compound **1** as the lead showed that the pyrazole ring at C-3 and the methyl group at

Table 1. Summary of Early SAR<sup>9</sup>



compd	X	R	$IC_{50}$ (nM)		
			Aur A	AurB	cell <sup>c</sup>
<b>1</b> <sup>b</sup>	Me	H	≤4	≤13	250
<b>2</b>	Et	H	≤4	≤13	850
<b>3</b>	H	H	≤4	≤13	1260
<b>4</b>	H	Me	568	258	ND <sup>c</sup>

<sup>a</sup> Inhibition of histone H3 phosphorylation in HCT-116 cells. <sup>b</sup> Kinetic solubility of compound **1** =  $5 \mu\text{M}$ . <sup>c</sup> ND: not determined.

C-6 were optimal.<sup>9</sup> Small nonpolar groups were preferred at C-6 with the methyl group (**1**), improving cell penetration over the close analogues such as **2** and **3** (Table 1). Alkylation of the pyrazole at C-3 resulted in significant loss of binding (**3** vs **4**). This indicated that the pyrazole NH may be

Received Date: March 31, 2010

Accepted Date: May 14, 2010

Published on Web Date: June 07, 2010

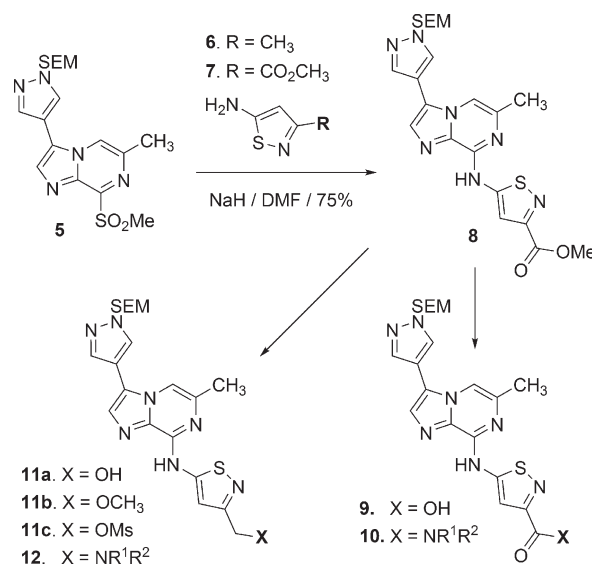
interacting with an H-bond acceptor of a side chain in the binding pocket. Indeed, the X-ray structure of compound **3** bound in the ATP binding pocket of Aurora A kinase domain showed that the pyrazole NH interacts with Asp 274 and that N1 and the 8-NH group are bound to Ala 213 in the hinge region.<sup>9</sup> The molecule seems to be locked into the binding conformation by the back bonding of the sulfur *d*-orbital with the lone pair on N7; the isothiazole ring is needed to facilitate this interaction. Thus, we decided to leave the C-3 and C-6 substituents intact for our lead optimization efforts and focus on the isothiazole ring. As the methyl substituent on the isothiazole is pointing toward the solvent region,<sup>9</sup> we rationalized that installation of polar groups such as alcohols, ethers, amides, and amines in this vicinity would be tolerated as the polar group would be solvent exposed. The polar group would also modulate the physicochemical properties of the lead and might improve cell penetration and water solubility.

The lead compound **1** was made via the displacement of the 8-methane sulfonyl group in the imidazo-[1,2-*a*]-pyrazine core<sup>10</sup> intermediate **5** with commercially available 5-amino-3-methyl isothiazole (**6**).<sup>9</sup> To execute our strategy of installing polar functionality on the isothiazole, we needed 5-amino isothiazole-3-methyl carboxylate (**7**), which was prepared in a multigram quantity by adapting a literature procedure.<sup>11</sup> With the functionalized isothiazole **7** in hand, we turned our attention to the design and preparation of target compounds outlined in our strategy (Scheme 1).

The coupling of compound **7** to the core intermediate **5** worked better than that of **6** presumably due to the stabilization of the amine anion afforded by the ester. The ester (**8**) was hydrolyzed to the carboxylic acid (**9**) and coupled with various amines to form the amides (**10**). Alternatively, methyl ester was reduced to the alcohol **11a** and converted to methyl ether **11b**. Activation of the alcohol to the mesylate **11c** and displacement with various amines provided the targets **12**. Removal of the SEM protecting groups completed the synthesis of target compounds for testing as amorphous HCl salts.

All of our compounds were first evaluated in the biochemical assay, and IC<sub>50</sub> values were determined by assessing the ability of the compound to inhibit the phosphorylation of peptide substrates by Aurora kinases A and B. This assay had detection limits of  $\geq 4$  nM for Aurora A and  $\geq 13$  nM for Aurora B. Potent binders of Aurora A and B were then tested in mechanistic cell-based assays. Aurora B-mediated phosphorylation of Histone H3 at Ser 10 (phos-HH3) was measured by immunofluorescence following the treatment of nocodazole synchronized HCT 116 cells with the Aurora inhibitor. The potency of phos-HH3 inhibition was expressed as IC<sub>50</sub> values. Small molecule inhibition of Aurora A and B causes mitotic arrest leading to abrogation of cytokinesis, resulting in a cell with 4N DNA. As the undivided cells continue through the cell cycle (endoreduplication), they accumulate > 4N DNA content.<sup>3</sup> Following compound treatment, the DNA content of cells was measured by flow cytometric analysis. The result of this assay was expressed as the minimum concentration (C<sub>min</sub>) of the compound required for inducing endoreduplication in asynchronous cells. Thus, the two mechanistic cell-based assays directly assessed target engagement in vitro.

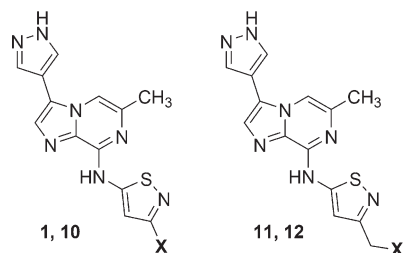
Scheme 1. Synthesis of Target Compounds



In general, more polar substituents did not affect binding potency (Table 2), but their polarity had to be modulated to improve cell potency. The methyl ester **8**, the carboxylic acid **9**, and the equally polar primary (**10a**, X = CONH<sub>2</sub>), secondary (**10b**, X = CONHMe), and acyclic tertiary (**10c**, X = CONMe<sub>2</sub>) carboxamides had no effect in cells (phos-HH3 > 10  $\mu$ M), but cyclic tertiary amides with increasing lipophilicity started registering cell-based activity. Thus, the piperidine carboxamide **10f** (log *P* = 2.5) nearly matched the cell potency of the simple methyl isothiazole **1** (log *P* = 2.7), indicating that polar groups would be tolerated in this region of the inhibitor.

Since improving the water solubility of the target compounds was also one of the objectives in introducing a polar substituent in the solvent-exposed region of the molecule, we also evaluated the alcohol and amines (Table 2), as these derivatives are usually more soluble in aqueous medium. The cell-based activity of the more lipophilic tertiary amines (**12c–k**) was 5–10-fold higher than the tertiary amide **10f**, indicating a preference for the sp<sup>3</sup> carbon as the linker between the isothiazole ring and the polar group at the solvent front. The cell potency of the cyclic amines increased with ring size (**12d,e,h**). Introduction of a heteroatom in the ring (**12f,g**) was detrimental for cell potency. The acyclic amine **12c** showed higher cell potency than its cyclic counterparts (**12d,e**), and  $\alpha$ -substitution (**12i**) seemed to tweak the cell potency further. Adding more polar ether (**12j**) and alcohol (**12k**) groups did not affect the cell potency of acyclic amines but improved their aqueous solubility.

Structures of two other target compounds **13** and ( $\pm$ )-**14** made to address the effect of the linker length are shown in Figure 1, and their synthesis is described in the Supporting Information section. Compounds **13** and **14** had IC<sub>50</sub> values of 35 and 149 nM, respectively, in the cell-based phos-HH3 inhibition assay. Thus, the homologue **13** had slightly improved cell potency over the methylene-linked **12e**, but the solubility of **13** was also slightly reduced. Constraining the carbon linker between the isothiazole and the amine in the

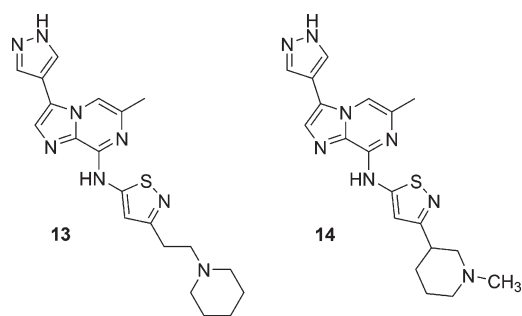
**Table 2.** Effect of Polar Groups on Cell Potency

Comp	R	IC <sub>50</sub> (nM)		
		Aur A	Aur B	phos-HH3
<b>1</b>	CH <sub>3</sub>	≤ 4	≤ 13	<b>250</b>
<b>10d</b>		≤ 4	≤ 13	860
<b>10e</b>		≤ 4	≤ 13	620
<b>10f</b>		≤ 4	≤ 13	<b>300</b>
<b>11a</b>	OH	≤ 4	≤ 13	797
<b>11b</b>	OCH <sub>3</sub>	≤ 4	≤ 13	440
<b>12a</b>	NH <sub>2</sub>	≤ 4	≤ 13	1260
<b>12b</b>		≤ 4	≤ 13	364
<b>12c</b>		≤ 4	≤ 13	35
<b>12d</b>		≤ 4	≤ 13	87
<b>12e</b>		≤ 4	≤ 13	50
<b>12f</b>		≤ 4	≤ 13	250
<b>12g</b>		≤ 4	≤ 13	412
<b>12h</b>		≤ 4	≤ 13	<b>18</b>
<b>12i</b>		≤ 4	≤ 13	<b>20</b>
<b>12j</b>		≤ 4	≤ 13	<b>26</b>
<b>12k</b>		≤ 4	≤ 13	<b>24</b>

form of a ring (**14**) was detrimental for cell potency and did not warrant the separation of its pure enantiomers.

Since improving aq solubility toward iv administration was also our criteria, the solubility of the compounds in Table 3 was initially estimated in a high-throughput kinetic solubility assay<sup>12</sup> at pH 7.4. The solubility of cyclic amines was typically in the 50–100 μM range (**12h** = 125 μM), and for acyclic amines, it was 250 μM (limit) in this assay. The installation of tertiary amines via a methylene linker on the isothiazole improved cell potency by 5–10-fold and also increased solubility by 10–50-fold over the initial lead **1**, thus validating our design strategy.

All compounds (**12h–k**) with phos-HH<sub>3</sub> IC<sub>50</sub> < 30 nM were also potent inducers of endoreduplication (Cmin ~ 16 nM; FACS analysis) in hyper proliferating HCT116 cells, which further confirmed target engagement. The cell proliferation data showed that the compounds were very potent inhibitors of cell growth, with IC<sub>50</sub> values of 2, 4, 7 and 6 nM respectively for **12h–k**. Thus these four compounds

**Figure 1.** Compounds designed to address linker length.**Table 3.** Therapeutic Index and Equilibrium Solubility Data

Comp	Amine	phos-HH3 IC <sub>50</sub> (nM)	MED mg/kg	MTD mg/kg	Sol* mg/ml
<b>12h</b>		18	3	>100	0.01
<b>12i</b>		20	6	>100	0.13
<b>12j</b>		<b>26</b>	<b>13</b>	<b>&gt;100</b>	<b>5.1</b>
<b>12k</b>		<b>25</b>	<b>2.5</b>	<b>&gt;100</b>	<b>5.7</b>

\*Equilibrium solubility, citrate buffer (pH 5.3).

**12h–k** were indistinguishable in terms of their cell potency profile.

In order to differentiate the top compounds (**12h–k**) with promising combination of cell potency (phos-HH<sub>3</sub> IC<sub>50</sub> ~ 25 nM) and kinetic solubility (≥ 125 μM), each compound was progressed to a PD/PK study to determine its therapeutic index as well as an equilibrium (thermodynamic) solubility study under buffered conditions to determine if the compound had the high solubility required for an intravenous drug. The results of this study for the four compounds are summarized in Table 3.

In the PD/PK study, the target compound (50, 10, 2.5 mg/kg, ip) was dosed in A2780 tumor bearing mice, and at 1 hr post-dose phos-HH<sub>3</sub> levels were determined. The minimum efficacious dose (MED) was defined as the dose which inhibited phos-HH<sub>3</sub> levels by 50% at 1 hr post dose. The plasma concentration of the compound at the 1 hr time point was taken to correlate the observed PD response with exposure level. The maximum tolerated dose (MTD) was defined as the dose below the dose that caused ≥ 20% body weight loss or lethality. For the MTD study nude mice were dosed with the compound (50, 75 and 100 mg/kg, ip) 2x week.

Drugs that are administered intravenously require solubility in the millimolar (mM) range. Clearly, compounds **12h** and **12i** did not meet the solubility criteria. The amino ether **12j** and the amino alcohol **12k** had similar levels of intrinsic solubility (> 5 mg/mL), but the MED for the amino ether **12j** was 4-fold higher than that of **12k**. The amino alcohol **12k** had the best combination of therapeutic index and equilibrium

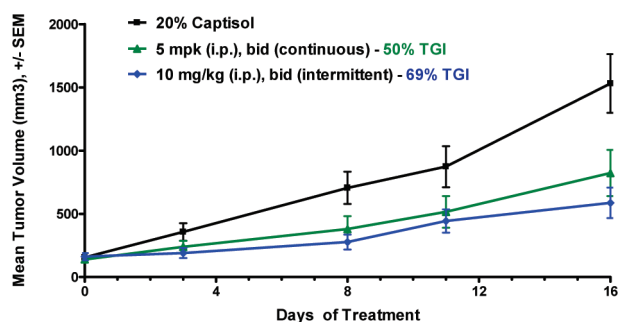


**Figure 2.** Efficacy study of **12k** in A2780 human tumor xenograft model in mouse ( $n = 10$ ) as measured by median tumor volumes (cubic mm). Captisol (20%; vehicle control) (black square), 5 mg/kg (i.p.) bid dosed daily on days 0–16 (TGI = 50%) (green triangle), and 10 mg/kg (i.p.) bid dosed intermittently on days 0–4 and 10–14 (TGI = 69%) (blue diamond). Error bars: standard error of the mean ( $\pm$ SEM).

solubility. The PK arm of the study showed that **12k** gave its PD response at a concentration of 110 nM ( $C_{1h}$ , 2.5 mg/kg, ip), which reflects a reasonable exposure ( $4\times$ ) over its  $IC_{50}$  value of 25 nM in the cell-based phos-HH3 assay.

Compound **12k** was evaluated for its efficacy in A2780 human tumor xenograft model in mouse as a single agent (Figure 2). For example, a low dose of 5 mg/kg (ip, bid) was well-tolerated in a continuous dosing schedule and showed 50% tumor growth inhibition (TGI) on day 16. A higher dose of 10 mg/kg (ip, bid) was well-tolerated in an intermittent schedule (5 days on, 5 days off) and gave 69% TGI on day 16. Neither body weight loss nor lethality was noted in both treatment groups.<sup>15</sup>

The X-ray cocrystal structure of the amino alcohol **12k** bound in the ATP binding pocket of Aurora A is shown in Figure 3. As seen with the earlier compound **3**,<sup>9</sup> this molecule is anchored via the binding of N1 and 8-NH groups to Ala 213 in the hinge region, with the H-bonding between the 3-pyrazole NH and Asp 274 contributing to its specificity for this target. Additionally, the second pyrazole N interacts with a bridging water molecule. The amine points toward the solvent-exposed front of the binding pocket, and its rotational freedom is restricted by intramolecular bonds formed by the 3° amine with the alcohol and the isothiazole (N).

Direct binding of **12k** to the kinase domains of Aurora kinases A and B was further confirmed by temperature-dependent fluorescence (TdF) study,<sup>15,16</sup> with  $K_d$  values of 0.02 (Aur A) and 0.03 nM (Aur B). Kinase counter screens demonstrated that this compound also inhibited the Src family of kinases ( $IC_{50} < 10$  nM), Chk1 ( $IC_{50} = 13$  nM), VEGFR2 ( $IC_{50} = 1$  nM), and IRAK4 ( $IC_{50} = 37$  nM). It did not have significant activity ( $IC_{50} > 1000$  nM) against 34 other kinases representing different families of the kinome.<sup>17</sup>

The pharmacokinetic parameters of the amino alcohol **12k** (amorphous 2HCl salt), administered intravenously, in four different species are summarized in Table 4. The compound showed good exposure in all species with the clearance being high in rodents and moderate in dog and monkey. The half-life was also moderate, but the tissue distribution was high.

Compound **12k** was only moderately bound to plasma proteins. At a concentration of 10  $\mu$ M **12k**, protein binding

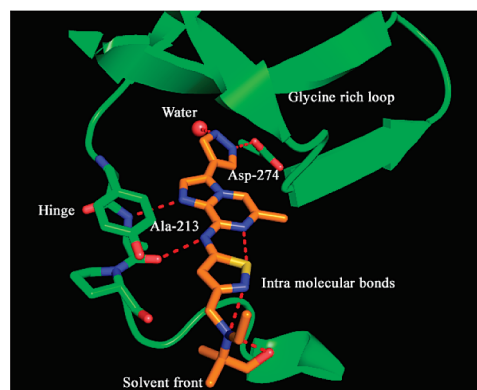


**Figure 3.** X-ray cocrystal structure of **12k** bound in Aurora A.<sup>14</sup>

**Table 4.** PK Parameters of **12k** (Intravenous Administration)

species	AUC <sub>0-∞</sub> (μM h)	C <sub>max</sub> (μM)	T <sub>1/2</sub> (h)	Cl (mL/mi/kg)	Vd (SS) (L/kg)
mouse <sup>a</sup>	0.9		1	107	6.1
rat <sup>b</sup>	1.3	2	8.3	91	19
dog <sup>b</sup>	4.2	9.1	4.4	28	4.7
monkey <sup>b</sup>	7.5	7.4	7.4	16	4.2

<sup>a</sup> Dose = 2.5 mg/kg (20% HPBCD). <sup>b</sup> Dose = 3 mg/kg (20% Captisol/20 mM citrate buffer).

was 87% in rodents, 87% in dog, 84% in monkey, and 85% in human plasma, as determined in vitro by equilibrium dialysis. The major metabolic pathway for **12k** was N-deethylation with and without oxidation and glucuronidation, when the radiolabeled compound was incubated at 37 °C for 24 h with cryo-preserved mouse, rat, dog, monkey, and human hepatocytes.<sup>18</sup> All of the metabolites observed from human hepatocytes were also observed in other species. In human liver microsomes, the  $IC_{50}$  values were  $>30$   $\mu$ M for the inhibition of Cyp enzymes 1A2, 2C8, 2C9, 2C19, 3A4, and 2D6 (co-incubation 2D6:  $IC_{50} = 14$   $\mu$ M), suggesting that compound **12k** is unlikely to cause inhibitory drug–drug interactions when coadministered with other drugs that are metabolized by these enzymes. In the mini-Ames assay, **12k** did not show any potential for mutagenicity. In the voltage clamp assay, **12k** showed 38% inhibition of the hERG potassium channel at a concentration of 6  $\mu$ M. However, the compound did not show any adverse cardiovascular effects at therapeutic concentrations in a safety pharmacology study in dogs.

In conclusion, optimization of the lead structure **1** by installation of polar groups in the solvent-exposed region of the inhibitor led to the identification of the amino-alcohol **12k** (SCH 1473759) as a novel, picomolar inhibitor of Aurora kinases A and B with high intrinsic aqueous solubility (11 mM). It has acceptable PKs for an iv administration, on target efficacy, and a safety profile suitable for further evaluation. The template embedded in the structure of **12k** is very versatile and has also given rise to other Aurora kinase inhibitors that have oral bioavailability as well as high cell potency. These studies will be reported in due course.

**SUPPORTING INFORMATION AVAILABLE** Experimental procedures for the preparation of compounds **7**, **8**, **10f**, **12h–k**, and **13–14** and the biological assays described herein. This material is available free of charge via the Internet at <http://pubs.acs.org>.

**Accession Codes:** The coordinates for **12k** have been deposited with the RCSB Protein Data Bank under the code 3MYG.

#### AUTHOR INFORMATION

**Corresponding Author:** \*To whom correspondence should be addressed. E-mail: [jayaram.tagat@merck.com](mailto:jayaram.tagat@merck.com).

**ACKNOWLEDGMENT** We thank Drs. John Piwinski, Dan Hicklin, Paul Kirschmeier, Frederick Monsma, and W. Robert Bishop for their management. Dr. Jesse Wong (Discovery Synthesis Group) is thanked for supplying large amounts of compound **5**, and Dr. David Hesk is thanked for providing the  $^3\text{H}$ -SCH-1473759 (**12k**). Drs. Rumin Zhang (Protein Chemistry), Lucy Xu (Pharmacokinetics), Li-Kang Zhang (Mass Spectroscopy), Ronald Snyder (Ames assay), Steven Sorota (hERG data), and Alan Bass (Drug Safety) are gratefully acknowledged for their supporting studies. Drs. Mathew Voss and Matthew Rainka (Albany Molecular Research, Inc) are thanked for their collaboration in this project.

#### REFERENCES

- (1) Pollard, J. R.; Mortimore, M. Discovery and development of Aurora kinase inhibitors as anticancer agents. *J. Med. Chem.* **2009**, *52*, 2629–2651.
- (2) Cheung, C.-H. A.; Coumar, M. S.; Hsieh, H.-P.; Chang, J.-Y. Aurora kinase inhibitors in preclinical and clinical testing. *Expert Opin. Invest. Drugs* **2009**, *18* (4), 379–398.
- (3) Yang, H.; Burke, T.; Dempsey, J.; Diaz, B.; Collins, E.; Toth, J.; Beckmann, R.; Ye, X. Mitotic requirement for Aurora A kinase is by-passed in the absence of Aurora B kinase. *FEBS Lett.* **2005**, *579*, 3385–3391.
- (4) Aliagas-Martin, I.; Burdick, D.; Corson, L.; Dotson, J.; Drummond, J.; Fields, C.; Huang, O. W.; Hunsaker, T.; Kleinheinz, T.; Krueger, E.; Liang, J.; Moffat, J.; Phillips, G.; Pulk, R.; Rawson, T. E.; Ultsch, M.; Walker, L.; Wiesmann, C.; Zhang, B.; Zhu, B.-Y.; Cochran, A. G. A class of 2,4-bisanilino pyrimidine Aurora A inhibitors with unusually high selectivity against Aurora B. *J. Med. Chem.* **2009**, *52*, 3300–3307.
- (5) Mortlock, A. A.; Foote, K. M.; Heron, N. M.; Jung, F. H.; Pasquet, G.; Lohmann, J.-J. M.; Warin, N.; Renaud, F.; De Savi, C.; Roberts, N. J.; Johnson, T.; Dousson, C. B.; Hill, G. B.; Perkins, D.; Hatter, G.; Wilkinson, R. W.; Wedge, S. R.; Heaton, S. P.; Odedra, R.; Keen, N. J.; Crafter, C.; Brown, E.; Thompson, K.; Brightwell, S.; Khatri, L.; Brady, M. C.; Kearney, S.; McKillop, D.; Rhead, S.; Parry, T.; Green, S. Discovery, synthesis and in vivo activity of a new class of pyrazoloquinazolines as selective inhibitors of Aurora B kinase. *J. Med. Chem.* **2007**, *50*, 2213–2224.
- (6) Oslob, J. D.; Romanowski, M. J.; Allen, D. A.; Baskaran, S.; Bui, M.; Elling, R. A.; Flanagan, W. M.; Fung, A. D.; Hanan, E. J.; Harris, S.; Heumann, S. A.; Hoch, U.; Jacobs, J. W.; Lam, J.; Lawrence, C. E.; McDowell, R. S.; Nannini, M. A.; Shen, W.; Silverman, J. A.; Sopko, M. M.; Tangonan, B. T.; Teague, J.; Yoburn, J. C.; Yu, C. H.; Zhong, M.; Zimmerman, K. M.; O'Brien, T.; Lew, W. Discovery of a potent and selective Aurora kinase inhibitor. *Bioorg. Med. Chem. Lett.* **2008**, *18*, 4880–4884.
- (7) Ghose, A. K.; Herberich, T.; Pippin, D. A.; Salvino, J. M.; Mallamo, J. P. Knowledge based prediction of ligand binding modes and rational inhibitor design for kinase drug discovery. *J. Med. Chem.* **2008**, *51*, 5149–5171.
- (8) Zuccotto, F.; Ardini, E.; Casale, E.; Angiolini, M. Through the "Gatekeeper Door": Exploiting the active kinase conformation. *J. Med. Chem.* **2010**, *53*, 2681–2694.
- (9) Belanger, D.; Curran, P.; Hruza, A.; Voigt, J.; Meng, Z.; Mandal, A. K.; Siddiqui, M. A.; Basso, A.; Gray, K. The discovery of potent imidazo [1,2-*a*] pyrazines as aurora kinase inhibitors. *Bioorg. Med. Chem. Lett.* **2010**, submitted for publication.
- (10) Yu, T.; Belanger, D. B.; Kerekes, A. D.; Meng, Z.; Tagat, J. R.; Esposito, S.; Mandal, A. K.; Xiao, Y.; Kulkarni, B. A.; Zhang, Y.; Curran, P. J.; Doll, R. J.; Siddiqui, M. A. Imidazo pyrazines as protein kinase inhibitors and their preparation and use in the treatment of kinase mediated diseases. *PCT Int. Appl.* (**2008**), 156614 A2, pp 287, WO.
- (11) Walsh, R. J. A.; Wooldridge, K. R. H. Isothiazoles XV: 5-Nitroisothiazoles. *J. Chem. Soc., Perkin Trans. 1: Org. Bio-Org. Chem.* **1972**, 9–10, 1247–1249.
- (12) Kinetic solubility was determined in 10 mM sodium phosphate, pH 7.4, 2% DMSO by a static light scattering method using NepheloStar (BMG LabTech, Durham, NC).
- (13) Additional studies: Basso, A. D.; Gray, K.; Tevar, S.; Ponery, S.; Lee, S.; Liu, M.; Smith, E.; Yu, T.; Tagat, J.; Doll, R.; Kerekes, A.; Belanger, D.; Siddiqui, A.; Zhang, Y.; Xiao, Y.; Esposito, S.; Monsma, F.; Hicklin, D.; Kirschmeier, P. *SCH 1473759, a Novel Aurora Inhibitor, Demonstrates Enhanced Antitumor Activity in Combination with Taxanes and KSP Inhibitors*, 101st Annual Meeting of AACR, Washington, DC, April 17–21, **2010**; Poster 1648.
- (14) Figure 3 was generated using PyMol: DeLano, W. L. *The PyMOL Molecular Graphics System*; DeLano Scientific: Palo Alto, CA, 2002.
- (15) Langsdorf, E. F.; Malikzay, A.; Lamarr, W. A.; Daubaras, D.; Kravec, C.; Zhang, R.; Hart, R.; Monsma, F.; Black, T.; Ozbal, C. C.; Miesel, L.; Lunn, C. A. Screening for antibacterial inhibitors of the UDP-3-O-(R-5-hydroxymyristoyl)-N-acetyl glucosamine deacetylase (LpxC) using a high throughput mass spectrometry assay. *J. Biomol. Screening* **2010**, *15*, 52–61.
- (16) Zhang, R.; Monsma, F. Fluorescence based thermal shift assays. *Curr. Opin. Drug Discovery Dev.* **2010**, in press.
- (17) Kinase selectivity: See the Supporting Information for a listing of the 34 kinases that were not inhibited by **12k**. Src kinase inhibition does not play a role in the phosphorylation of Histone H3 or in endoreduplication. Compound **12k** gave a dose proportional endoreduplication profile (FACS analysis), even at higher concentrations, with no interference from off target effects on the observed Aurora B phenotype.
- (18) After incubation with hepatocytes for 24 h, the des-ethyl metabolite was formed in higher amounts as compared to other metabolites, but the parent compound **12k** was still the major product. A pure sample of the des-ethyl metabolite of **12k** did not have cell-based activity (pHH3 inhibition  $\text{IC}_{50} > 1000$  nM), precluding any contribution from this metabolite to the observed in vivo data.